(230.0230) Optical devices ; (300.6495) Spectroscopy, terahertz.

Highly sensitive terahertz dielectric sensor for low-volume liquid samples

A. Soltani,[1] H. Neshasteh,[2] A. Mataji-Kojouri,[2] N. Born,[1] E. Castro-Camus,[3,*] M. Shahabadi,[2] and M. Koch[1]

[1] *Faculty of Physics and Material Sciences Center, Philipps-Universität Marburg, Renthof 5, 35032 Marburg, Germany*

[2] *Photonics Research Lab., Center of Excellence for Applied Electromagnetics Systems, School of Electrical and Computer Engineering, University of Tehran, Tehran, Iran.*

[3] *Centro de Investigaciones en Optica A.C., Loma del Bosque 115, Lomas del Campestre, Leon, Guanajuato 37150, Mexico*

We present a waveguide based sensor for the measurement of the refractive index of dielectric liquid samples. The proposed sensor operates on the basis of an electromagnetic resonance between a thin metallic grating and a reflecting ground plane. The fluid whose refractive index is to be measured, fills the region between the metallic grating and the ground plane and causes a considerable shift in the resonance frequency (>500 GHz/RIU). The sensor has a relatively simple structure, therefore, it can be manufactured economically on industrial scales.

After three decades of intensive research and development the applicability, at least in principle, of terahertz spectroscopy [1, 2] has been demonstrated in science [3–6] industrial technology [7–9] and other disciplines [10–13]. Yet the "real-world" applicability of this technique, particularly in industry, is limited because of two reasons. Firstly, the cost of spectrometers is relatively high which is an issue that is being addressed by the community [14–16]. Secondly, the availability of high-sensitivity devices is limited. Recently, publications by Mendis *et al.*[17] and Ng *et al.*[18] presented clever approaches for the design and fabrication of a terahertz waveguide sensor and a plasmonic sensor respectively. Those devices show resonances caused by their geometries that shift in frequency at a rate of ∼91 GHz/RIU (refractive-index-unit) and ∼500 GHz/RIU. Another approach recently introduced was the use of split-ring-resonator metasurfaces which showed a sensitivity of ∼270 GHz/RIU for refractive index changes from 1 to 1.4 and extremely high sensitivities (∼1500 GHz/RIU) for small refractive index changes around 1.44 [19] with potential applicability in the fuel industry. Additionally, dielectric waveguide based sensors have been reported [20–22]. In this article, we present the design and characterization of a device featuring a sensitivity above 500 GHz/RIU across the entire $1.2< n <1.6$ range which is comparatively economical to produce and which requires only ∼150μl of the liquid under study, making it viable for large scale production, as well as clinical or industrial applications.

In order to design our resonant device, a numerical method for scattering analysis of multilayer periodic structures was used [23–25]. This approach is a frequency-domain semi-analytical algorithm based on a pseudo-Fourier expansion of the electromagnetic fields in a multilayer periodic structure in the presence of an incident plane wave. In comparison to finite-difference methods, this approach can be used to model multilayer structures with very small features without requiring any fine numerical meshes, and therefore avoiding the computational cost in terms of memory and computation time. In this transmission-line formulation, a pseudo-Fourier expansions of electromagnetic fields is assumed as a solution to the Maxwell's equations. This leads to an infinite set of equations in the form of transmission-line equations for a multiconductor transmission line. In Fig. 1a, a schematic of the proposed sensor is shown. In each layer of the structure an eigenvalue problem should be solved in order to calculate different modes and their corresponding propagation constants. It is possible to demonstrate that this problem can be reduced to a transmission-line network where each mode corresponds to a transmission line. At the interfaces between two successive layers, the continuity condition of the transverse electromagnetic fields is ensured by proper interconnection of transmission lines. Note that this method can accurately predict the electromagnetic field everywhere inside the sensor. The proposed sensor structure shows a resonance, at which, the incident radiation couples into the waveguide formed between two metallic layers. The radiation at other frequencies is reflected off the sensor. The resonance frequency is dependent on the refractive index of the material filling the volume between the metallic surfaces.

The schematic of the device with dimensions and the geometry of the experiment are shown in Fig. 1a and b. The sensor is made of two pieces of aluminium which are kept in contact, shown separated in the schematic in Fig. 1a for clarity. The top layer of the device is a 10 μm thick piece of aluminium foil where 220 μm parallel grooves were fabricated by laser machining. The grooves are separated by 330 μm strips of metal. The bottom piece of the sensor is a block of aluminium with a 10 μm deep planar cavity. When the two parts are placed in contact at the edges, the foil piece remains freestanding in the center with a separation of 10 μm from the second part. Some of the authors of this article recently introduced the calculations for a similar design during

* Corresponding author: enrique@cio.mx

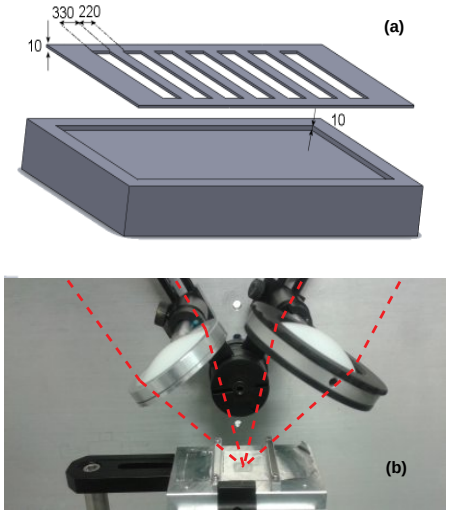

FIG. 1. (a) Three-dimensional schematic of the device (all dimensions in the figure are in μm). The device consists of a depleted plane aluminium cavity with a depth of 10 μm over which a periodic groove structure fabricated on 10 μm thick aluminium foil is located. The grooves are 220 μm wide, spaced by 330 μm metallic strips. (b) A photograph of the device in the experiment. The terahertz radiation from a photoconductive emitter is focused onto the device at -30° by a polyethylene lens, subsequently the reflection at +30° is collected by a second lens and directed to the detector. Dashed lines were added in order to illustrate the terahertz radiation trajectory.

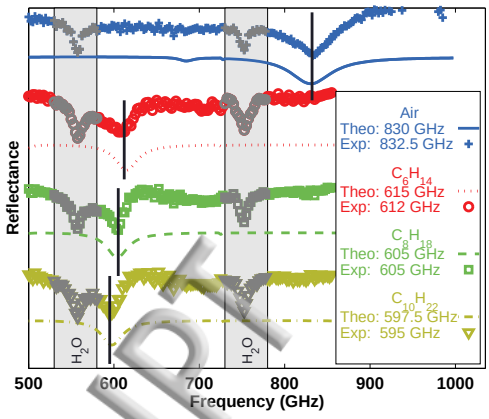

FIG. 2. From top to bottom, the first two curves shown (crosses and continuous line) represent the experimental measurement and theoretical calculation of the device in the absence of liquid sample (ie. for air). Analogously, the following two (circles and dotted line) correspond to hexane (n=1.370). The next two (squares and dashed line) are for octane (n=1.391). The final two (triangles and dash-dotted line) are for decane (n=1.405) [27]. Continuous lines on top of the experimental data are provided as a guide-to-the-eye only. Vertical lines were added at the center frequency of the experimental resonances for comparison. The areas shaded in gray correspond to windows of poor atmospheric transmission caused by water vapour; therefore, the additional resonances in these regions are not associated with the device.

a conference [26]. The structure has a resonance that is highly sensitive to the refractive index of the material filling the space between the top and bottom pieces. Given that the thin aluminum foil piece is relatively fragile, it is worth mentioning that further calculations (not shown) demonstrate that variations of up to $\sim$10 μm in the periodicity of the thin film grooves produce negligible changes in the performance of the device. In order to verify the resonance behavior and the possible applicability as a high-sensitivity platform for terahertz refractive index measurements, the reflectance of the device was measured for air, hexane (C_6H_{14}), octane (C_8H_{18}) and decane ($C_{10}H_{22}$) filling the cavity. These are well characterized THz-transparent liquids [27].

The measurements were performed using a terahertz time-domain spectrometer based on an Er:fiber mode-locked laser. The laser produces optical pulses at a central wavelength of 1550 nm with a repetition rate of 80 MHz and a duration of $\sim$65 fs. The laser beam is divided into two arms, one of which is coupled into a fiber that guides it to a photoconductive emitter, which converts the optical pulses into single-cycle electromagnetic transients with a spectrum spanning across the terahertz band. The transients were then focused by a polystyrene lens onto the device at an incidence angle of 30° with p-polarization. The pulses where then reflected off the surface of the device shown in Fig. 1b. The reflected radiation was collimated by an additional polyethylene lens and subsequently focused onto a photoconductive detector. The second part of the optical beam is sent to a opto-mechanical delay line. Subsequently, it is also fiber coupled in order to guide it onto the photoconductive detector mentioned earlier. This second optical pulse gates the detector in order to record the terahertz transient's electric field as a function of the delay line position. In this way, the time-dependent waveform of the electromagnetic transients is recorded. The waveform can subsequently be Fourier transformed in order to obtain its spectrum.

The measurement results are shown in Fig. 2. The figure shows the spectral reflectance of the device measured in the presence of air (crosses). Afterwards the device was tested in the presence of hexane (circles), octane (squares) and decane (triangles). For each measurement, we added $\sim$150 μl of each one of the substances on a dry device. In addition, a series of curves, right under each experimental measurement, show the theoretically calculated spectral response. Vertical lines are shown at the experimentally measured center frequency of the resonances. As seen in the graph, there is an almost perfect correlation between the measurement and the calculation. The values are given in the right-hand side of the plot. Note that all the experimental and their corresponding theoretical values differ less than 3 GHz, which is consistent with the experimental spectral resolution

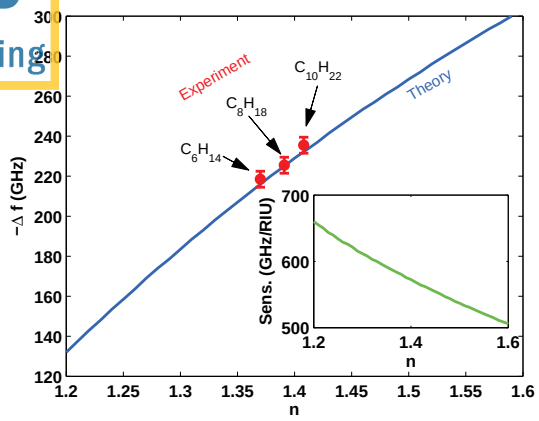

FIG. 3. The figure shows a continuous line which is the predicted frequency shift for the device frequency as a function of the refractive index of the liquid applied on it. The three points correspond to the experimentally measured frequency shifts for hexane, octane and decane. The inset shows the sensitivity of the device which exceeds 500 GHz/RIU in the region for refractive indices below 1.6.

of 2.5 GHz. Fig. 3 shows the frequency shift as a function of the refractive index with respect to the resonance in air (n=1). The points with error-bars correspond to the three alkanes measured. This allows us to estimate that the uncertainty for the refractive index would be $\sim \pm 0.01$ RIU when estimated from the resonant shift. Note the excellent agreement between the measured and the predicted frequency shifts. The inset of Fig 3 shows the sensitivity calculated from the theoretical curve. The sensitivity remains higher than 500 GHz/RIU in the entire range of refractive indices between 1.2 and 1.6, which corresponds to the refractive index region of the majority of transparent liquids. The main limitation of this scheme is that it is inappropriate for absorbing liquids such as water, which produce a broadening or complete disappearance of the resonance.

In this article, we presented the design, modeling, fabrication and characterization of a terahertz refractive index sensor for liquids. It shows excellent sensitivity (> 500 GHz/RIU) and requires very small amounts of sample (~150 μl). Its low-cost industrial production is feasible, given that it involves structural features in the hundreds of microns, which can easily be achieved by laser machining or low resolution photolithography; therefore, the device can even be manufactured as a single-use medical sensor or in the liquid chemical industry. We strongly believe that this device can be very useful in industrial characterization of fluids in the future.

The authors would like to thank the financial support of CONCyTEG (CFINN140810153004) and CONACyT (252939). Amin Soltani acknowledges funding from the German Academic Exchange Service (DAAD)

[1] A. Mitsuishi, Journal of Infrared, Millimeter, and Terahertz Waves **35**, 243 (2014).
[2] P. U. Jepsen, D. G. Cooke, and M. Koch, Laser & Photonics Reviews **5**, 124 (2011).
[3] B. Fischer, M. Hoffmann, H. Helm, G. Modjesch, and P. U. Jepsen, Semiconductor Science and Technology **20**, S246 (2005).
[4] E. Castro-Camus, M. Palomar, and A. Covarrubias, Scientific reports **3**, 2910 (2013).
[5] J. Lloyd-Hughes and T.-I. Jeon, Journal of Infrared, Millimeter, and Terahertz Waves **33**, 871 (2012).
[6] R. J. Falconer and A. G. Markelz, Journal of Infrared, Millimeter, and Terahertz Waves **33**, 973 (2012).
[7] P. Mousavi, F. Haran, D. Jez, F. Santosa, and J. S. Dodge, Appl. Opt. **48**, 6541 (2009).
[8] A. I. Hernandez-Serrano, S. C. Corzo-Garcia, E. Garcia-Sanchez, M. Alfaro, and E. Castro-Camus, Appl. Opt. **53**, 7872 (2014).
[9] T. Probst, S. Sommer, A. Soltani, E. Kraus, B. Baudrit, G. Town, and M. Koch, Journal of Infrared, Millimeter, and Terahertz Waves **36**, 569 (2015).
[10] K. Shiraga, Y. Ogawa, T. Suzuki, N. Kondo, A. Irisawa, and M. Imamura, Journal of Infrared, Millimeter, and Terahertz Waves **35**, 493 (2014).
[11] J. Labaune, J. B. Jackson, K. Fukunaga, J. White, L. d'Alessandro, A. Whyte, M. Menu, and G. Mourou, Applied Physics A **105**, 5 (2011).
[12] K. Krügener, M. Schwerdtfeger, S. Busch, A. Soltani, E. Castro-Camus, M. Koch, and W. Viöl, Scientific Reports **5**, 14842 (2015).
[13] M. Schwerdtfeger, S. Lippert, M. Koch, A. Berg, S. Katletz, and K. Wiesauer, Biomed. Opt. Express **3**, 2842 (2012).
[14] T. Probst, A. Rehn, and M. Koch, Opt. Express **23**, 21972 (2015).
[15] M. Scheller and M. Koch, Optics Express **17**, 17723 (2009).
[16] O. Morikawa, M. Tonouchi, and M. Hangyo, Applied Physics Letters **75**, 3772 (1999).
[17] R. Mendis, V. Astley, J. Liu, and D. M. Mittleman, Applied Physics Letters **95**, 171113 (2009).
[18] B. Ng, J. Wu, S. M. Hanham, A. I. Fernández-Domínguez, N. Klein, Y. F. Liew, M. B. Breese, M. Hong, and S. A. Maier, Advanced Optical Materials **1**, 543 (2013).
[19] J. Li, Z. Tian, Y. Chen, W. Cao, and Z. Zeng, Applied optics **51**, 3258 (2012).
[20] J.-F. Roux, F. Aquistapace, F. Garet, L. Duvillaret, and J.-L. Coutaz, Applied optics **41**, 6507 (2002).
[21] F. Aquistapace, L. Duvillaret, F. Garet, J.-F. Roux, and J.-L. Coutaz, Journal of applied physics **94**, 7888 (2003).
[22] Y. Laamiri, F. Garet, and J.-L. Coutaz, Applied Physics Letters **94**, 071106 (2009).
[23] M. A. Boroujeni and M. Shahabadi, Journal of Optics A: Pure and Applied Optics **8**, 856 (2006).
[24] M. A. Boroujeni and M. Shahabadi, Journal of Optics A:

Pure and Applied Optics **8**, 1080 (2006).
[25] See supplemental material at [URL will be inserted by AIP] for more information on the numerical method for scattering analysis of multilayer periodic structures..
[26] H. Neshasteh, A. Mataji-Kojouri, A. Soltani, and M. Shahabadi, in *Millimeter-Wave and Terahertz Technologies (MMWATT), 2014 Third Conference on* (IEEE, 2014) pp. 1–4.
[27] J. P. Laib and D. M. Mittleman, Journal of Infrared, Millimeter, and Terahertz Waves **31**, 1015 (2010).

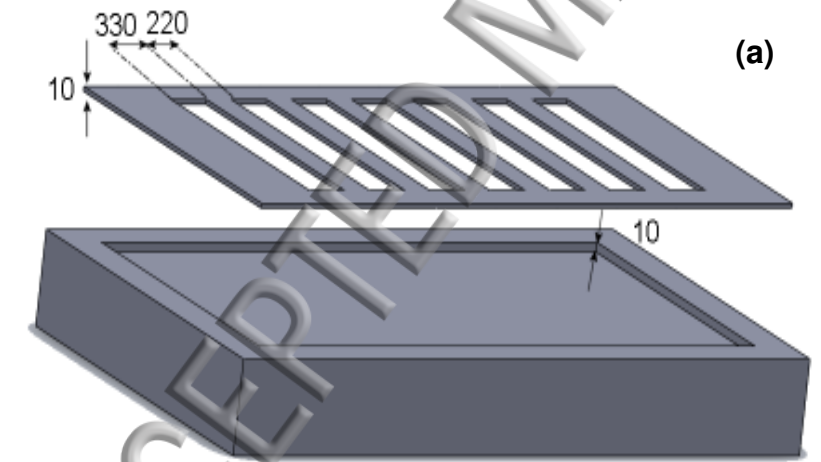

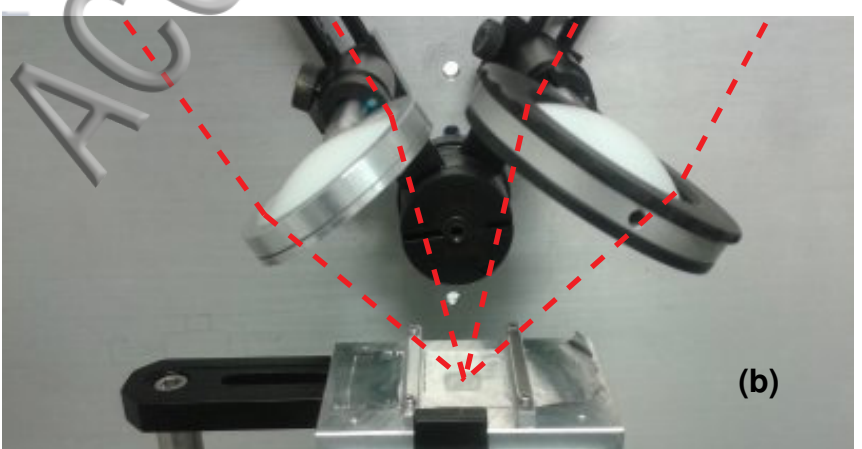

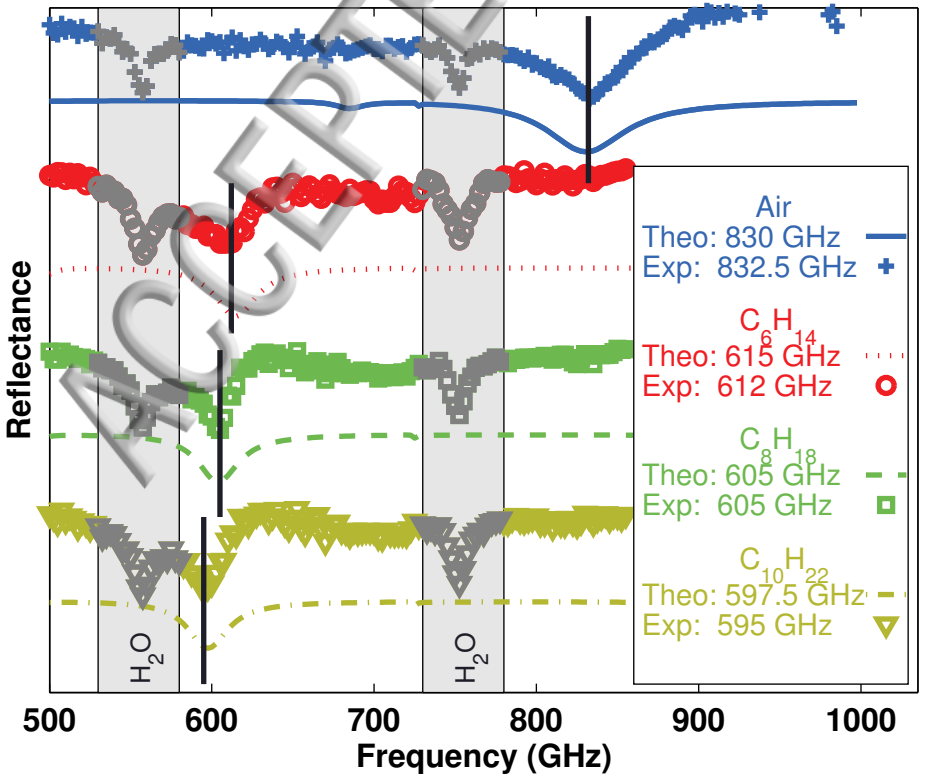
Reflectance
Frequency (GHz)
500
600
700
800
900
1000
H2O
H2O
Air
Theo: 830 GHz
Exp: 832.5 GHz
C6H14
Theo: 615 GHz
Exp: 612 GHz
C8H18
Theo: 605 GHz
Exp: 605 GHz
C10H22
Theo: 597.5 GHz
Exp: 595 GHz

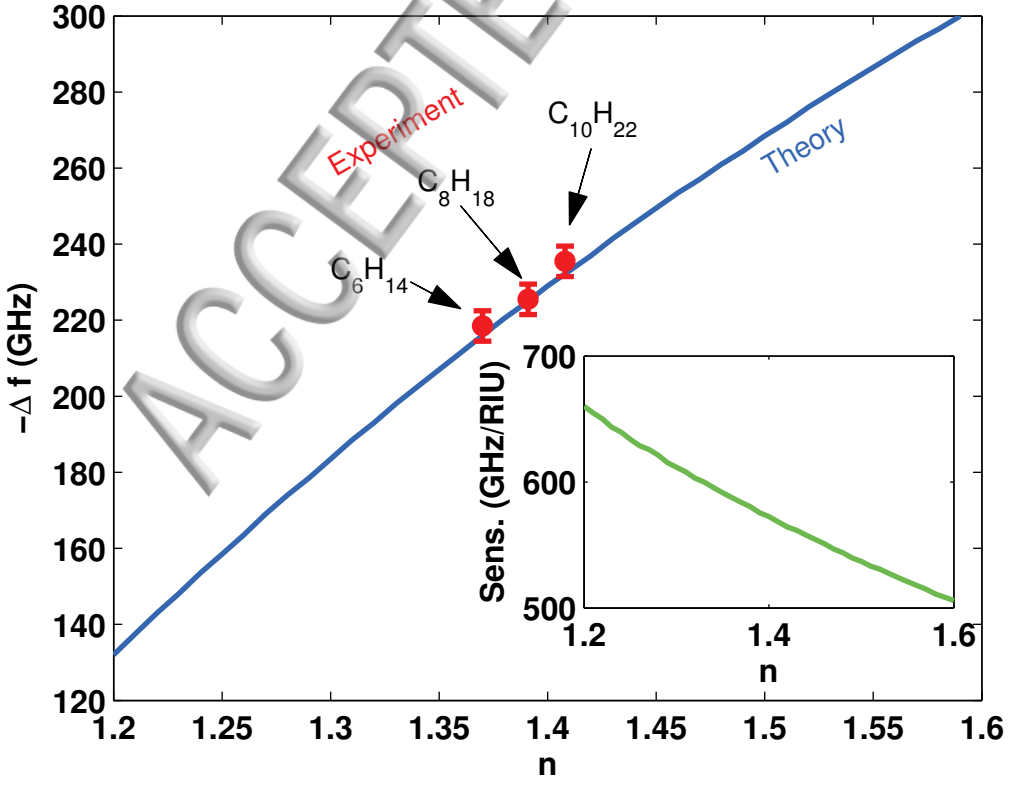
ACCEPTED
Experiment
Theory
$C_{10}H_{22}$
C_8H_{18}
C_6H_{14}
$-\Delta f$ (GHz)
n
Sens. (GHz/RIU)
n